CLM-P706

CLM-P706

UKAEA

Preprint

CULHAM LABORATORY
LIBRARY
27 APR 1984
b

DEVELOPMENTS OF MODELS FOR BOILING AND DRYOUT IN LIGHT-WATER REACTOR DEBRIS BEDS

K. A. MOORE
B. D. TURLAND

CULHAM LABORATORY
Abingdon Oxfordshire
1983

This document is intended for publication in a journal or at a conference and is made available on the understanding that extracts or references will not be published prior to publication of the original, without the consent of the authors.

Enquiries about copyright and reproduction should be addressed to the Librarian, UKAEA, Culham Laboratory, Abingdon, Oxon. OX14 3DB, England.

CLM-P706

DEVELOPMENTS OF MODELS FOR BOILING AND DRYOUT IN LIGHT-WATER REACTOR DEBRIS BEDS

K.A.Moore and B.D.Turland
UKAEA, Culham Laboratory,Abingdon,Oxon,OX14 3DB, U.K.

ABSTRACT

The coolability of solid self-heated fuel debris in water is a topic of major interest in probabilistic safety analyses of light-water reactors. Many experiments have been undertaken, using simulant heating methods and simulant materials for the particulate, to investigate the dependence of the dryout heat flux (i.e. that heating rate at which liquid coolant is no longer able to adequately penetrate the debris bed, such that local temperatures may rise considerably in excess of the coolant's boiling point). In most cases the observed dryout power is consistent with a semi-theoretical model developed by Lipinski*, and, in a slightly different form, by Turland and Moore**. The paper considers further developments and applications of these models. The particular topics discussed are (i) the transient approach to dry-out for deep beds, (ii) the effect of a gradation in particulate size (i.e. the mean particle diameter varies with position in the bed), and (iii) the inclusion of a dried-out layer in a one-dimensional model.

* Lipinski R.J. A model for boiling and dryout in particle beds. NUREG/CR-2646 (1982).

* Turland B.D, and Moore, Katharine. One dimensional models of boiling and dryout. In 'Post Accident Debris Cooling : Proceedings of the Fifth Post Accident Heat Removal Information Exchange Meeting, 1982' (Muller U, and Gunther C, eds), G.Braun (Karlsruhe), 192-197 (1983).

(Paper presented at International Meeting on Light-Water Reactor Severe Accident Evaluation, Cambridge, Mass., USA, September,1983).

September,1983.

1. INTRODUCTION

Particle beds of fuel debris, cladding and structural material may form in a number of circumstances during severe accident sequences hypothesised for light water reactors. For instance, for degraded core accidents in which core cooling is eventually restored, mainly solid debris in the core region may fragment if sufficient degradation has taken place. If core cooling is not restored molten debris is likely to contact water in the lower head and, should the vessel fail, also in the reactor cavity. In these circumstances the debris may be quenched and fragmented to form solid particulate. If there is a continuing supply of water to the debris, and the water can percolate throughout the debris bed the fission product heat may be removed by boiling water and the debris is said to be coolable; in these circumstances, provided containment integrity is maintained, the consequences to the public from the accident are likely to be insignificant [1,2] .

Many experiments [e.g. 3,4,5] with both water at 1 bar and simulant coolants have been undertaken to investigate the dryout heat flux of well-defined self-heated particulate (dryout is said to occur when liquid coolant is no longer able to reach some parts of the debris bed so that local temperatures may be considerably in excess of the boiling point of the coolant). Along with the experiments, correlations and mathematical models for the dryout heat flux have been developed. Models have the advantage that they can be validated against experiments with both simulant and real materials. The experiments showed that when the particle diameter was above about 1mm most of the particles remained fixed in the bed and thus a model based on flow through porous media was possible. Hardee and Nilson [6] produced a model in which the drag on each phase at a given liquid saturation was proportional to the superficial velocity (volume flux) of that phase, and in which liquid was drawn into the bed by gravity. The dryout flux was calculated by maximizing an expression in the saturation; the dryout heat flux was found to be independent of the depth of the layer. This original model was extended by the incorporation of drag terms that are quadratic in the superficial velocity rather than linear [7], and by the introduction of a saturation-dependent pressure difference (the 'capillary pressure') between the liquid and vapour phases [8,9,10]. This latter term gives a depth dependence of the dryout heat flux. The fullest description of the resulting model is given by Lipinski [9] who shows that reasonable agreement between the observed and predicted dryout power can be obtained for a wide range of coolants. It should be noted that the models described in [9] and [10] are based solely on conservation laws and phenomenological models of flow through porous media that were already well-established in the literature.

Although the models have been used primarily to estimate the dryout power, that of [9] also predicts the dependence of saturation on height in the steady state and can also be used to estimate the steady state thickness of the boiling region in a bed which is partially dried-out. The model development in [10] also retained transient terms in the conservation equations, thus allowing the prediction of the evolution of saturation with time. A summary of the model developed in [10] with some generalisations is given in section 2; the equations are presented in full vector form. It seems that a one-dimensional treatment is satisfactory for most boiling and dryout analyses; however it appears that this is not the case for experiments involving the quenching of hot solid particulate [11,12] where the same equations should apply. The higher dimensional equations will allow the validity of the 1-D models to be investigated.

The coolability of homogeneous debris beds is now well-understood, but experiments [e.g. 13]and model calculations by Lipinski [9] have shown that stratification of the debris or a gradation in particle size can have adverse effects on the coolability. This is investigated further in section 3.

For the analysis of accident sequences it is useful to be able to follow the transient behaviour of the debris, and calculate the steaming rate, and heat-up of the debris if it is uncoolable. So far it is only possible to make detailed transient predictions up to the onset of dryout. This is discussed in section 4 where the limit of no capillary pressure (usually implying large diameter particles)is examined. Qualitative comparisons are made with the experiments of Hofmann [14]. The inclusion of a dried-out layer is discussed in section 5 where a simple transient model is developed using steady state relations for the boiling region.

2. MODEL FOR A BOILING REGION OF A SELF-HEATED DEBRIS BED

2.1. General model equations

The model is restricted to that part of the debris bed which remains fixed. The debris bed is characterised by a porosity (ε) and a permeability (K) which may be functions of position.

Conservation of coolant mass implies

$$\varepsilon \frac{\partial}{\partial t} ((1-s)\rho_v + s\rho_\ell) + \nabla.(\rho_v U_v + \rho_\ell U_\ell) = 0 \quad (1)$$

where s is the liquid saturation, U denotes superficial velocity (volume flux per unit area), ρ denotes density, and the subscripts ℓ and v indicate liquid and vapour phases respectively.

The liquid and vapour phases are assumed to be in

equilibrium at the boiling point (non-equilibrium models are possible but these require a further heat transfer relationship). In this case a local heat balance implies

$$\varepsilon \frac{\partial}{\partial t}((1-s)\rho_v) + \underset{\sim}{\nabla}.(\rho_v \underset{\sim}{U}_v) = q/\lambda_{fg} \qquad (2)$$

where λ_{fg} is the latent heat of vaporization of the coolant. q is the heat source to the coolant per unit volume of bed; for boiling and dryout calculations it is the decay heat per unit volume, but it may also be calculated by an independent relation from the particle temperature (e.g. in quench modelling).

Equations of motion are written for the two coolant phase separately; these are based on the Ergun equation for a single phase and the concept of relative permeability [see 15 or 16 for a discussion of flow in porous media]. Subtracting these equations of motion one obtains

$$\frac{\rho_v \nu_v \underset{\sim}{U}_v}{\phi_v}\left[1 + \frac{0.01\ d}{(1-\varepsilon)\nu_v}|W_v|\right] - \frac{\rho_\ell \nu_\ell \underset{\sim}{U}_\ell}{\phi_\ell}\left[1+\frac{0.01\ d}{(1-\varepsilon)\nu_\ell}|\underset{\sim}{W}_\ell|\right]$$
$$= K\left[\underset{\sim}{\hat{z}}(\rho_\ell-\rho_v)g - \underset{\sim}{\nabla}(P_v - P_\ell)\right] \qquad (3)$$

where P denotes pressure, g the acceleration due to gravity, d the mean local particle diameter, ϕ the relative permeability and $\underset{\sim}{W}$ the pore velocity.

The pressure in the two phases are different, but related by the capillary pressure (P_c):

$$P_c = P_v - P_\ell = \sigma(\varepsilon/K)^{\frac{1}{2}}\ J(s) \qquad (4)$$

where σ is the surface tension and J(s) is a dimensionless function of saturation (the Leverett function).

2.2 One-dimensional form and dimensionless groups

For most applications (see above) the one-dimensional form of the equations is sufficient. Furthermore, the use of non-dimensional groups allows one to distinguish the important processes in a given experiment or application. To form the non-dimensionalization a typical heat flux density $\Phi_o = K_o(\rho_\ell-\rho_v)g\lambda_{fg}/\nu_v$ is defined (this is just the dryout heat flux from the simplified form of the Hardee-Nilson model); heights are scaled accordingly: $\xi = q_o z/\Phi_o$. The o subscript denotes a reference value.
Equations (1) - (4) can then be written in the form

$$\frac{\partial s}{\partial \tau} = \frac{\partial V_v}{\partial \xi} - \frac{q}{q_o} \qquad (5)$$

$$V_\ell + V_v = V^o + (1-BC)\int_o^\xi q(\xi^1)d\xi^1/q_o \qquad (6)$$

$$\frac{V_v}{f^2\phi_v}\left(1 + \frac{Af|V_v|}{1-s}\right) - \frac{V_\ell}{Cf^2\phi_\ell}\left(1 + \frac{Af|V_\ell|}{Bs}\right)$$
$$= 1 + \frac{EJ}{f^2}\cdot\frac{df}{d\xi} - \frac{E}{f}\frac{dJ}{ds}\frac{\partial s}{\partial \xi} \qquad (7)$$

for one-dimensional problems. $\tau = q_o t/(\varepsilon\rho_v L)$, $f = d/d_o$ gives the variation of mean particle diameter with height, and V^o is the (dimensionless) net flow of fluid into the bottom of the bed.

The dimensionless groups are $B = \nu_\ell/\nu_v$, $C = \rho_v\nu_v/(\rho_\ell\nu_\ell)$, $A = 0.01\ d\ \Phi_o/((1-\varepsilon)\rho_v\nu_v\lambda_{fg})$, $E = (\varepsilon K_o)^{\frac{1}{2}}\sigma q_o\lambda_{fg}/(\nu_v\Phi_o^2)$. A is a measure of the importance of the quadratic drag term, whilst E is a measure of the importance of capillary pressure. For water at 1 bar B = 0.0144 and C = 0.0434. Assuming the Kozeny form for the relative permeability [16] and $\varepsilon = 0.42$, for d_o = 1mm, Φ_o = 1.28MW m^{-2}, A = 0.81 and E = $9\times10^{-8}q_o$; if d_o = 3mm, Φ_o=11.5MW m^{-2}, A = 21.8 and E = $3.4\times10^{-9}q_o$ where q_o is in Wm^{-3}. A typical value of q_o for decay heat conditions is 2×10^6 (Wm^{-3}). At 100 bar values of Φ_o are multiplied by 23.9, of A by 23.6 and of E by 0.013.

Various forms of the phenomenological functions ϕ_v, ϕ_ℓ, J are available in the literature. For illustrative calculations the simplified forms of the relative permeability functions $\phi_v = 1 - s$ and $\phi_\ell = s^N$ where N = 1 (simple separated flow model) or N = 3 (better fit to data [15]) are used. The Leverett function used is

$$J(s) = 1.5 - 9.2s + 88s^2/3 - 880s^3/27 \quad (0 \le s \le 0.3)$$
$$= 0.62 - 0.4s \quad (0.3 \le s \le 0.8)$$
$$= 14.7 - 53.2s + 66s^2 - 55s^3/2 \quad (0.8 \le s \le 1)$$

which is based on data in [15].

3. STRATIFIED AND GRADED BEDS

Experiments [e.g. 13] have highlighted the possible adverse effects of a layer of fine particulate overlying a coarse layer; the dryout heat flux can be lower than that of the fine particulate alone. The steady state version of the model described above has been used for a number of sample calculations based on the parameters used in [13] for both layered and graded beds.

3.1. Two-layered beds

For layered beds an interface condition is required this is obtained by integrating equation [7] over a region of thickness δ spanning the interface. Taking the limit as the region of integration is decreased we obtain

$$E\left[\frac{J}{f}\right] = 0\ (\delta) \qquad (8)$$

where [J/f] denotes the jump across the interface. For a continuum model to be valid δ should cover many particles, thus $\delta >> dq_o/\Phi_o$. So provided that $d << E\ \Phi_o/q_o$, equation (8) implies

$$FJ(s_c) = J(s_f) \qquad (9)$$

where F is the ratio of the diameter of the fine particles to that of the coarse. s_c and s_f denote the limits of the saturation on the coarse and fine sides of the interface. Figure 1 shows a plot of s_f as a function of s_c and F. It is seen that large jumps in saturation can occur.

In the limit $E \to 0$ equation (9) is no longer applicable. A jump in saturation still occurs, but this is because the saturation at any height is now determined uniquely by the heat flux at that height and the local bed properties. If the latter change discontinuously so must the saturation. In the $E \to 0$ limit the dryout heat flux of a lower coarse

layer and an upper finer layer is just that of the finer layer irrespective of the distribution of internal heating.

Returning now to E non-zero, Figure 2 shows example calculationsfor uniform $q = 2 \times 10^6 Wm^{-3}$ for a coarse layer with particle diameter 0.004m, and a fine layer with particle diameter 0.0012m(the particle diameters chosen here have no significance other than that they were used in [13]). The purpose of Figure 2 is to identify those combinations of coarse and fine layer thickness that are just coolable by boiling. First, a series of steady-state plots (solid lines) of saturation against height are constructed for fine layers of varying thickness, including cases which would have dried-out regions (i.e. the saturation is zero at finite height).

Secondly the steady-state saturation profile for the deepest layer of coarse particles that can be cooled without dryout is constructed. Part of this is illustrated by the line consisting of dashes from the origin. We use this line which shows potential values of s_c when the coarse layer is just coolable by boiling, to construct a further curve using equation (9) which shows the possible values of liquid saturation at the bottom of the fine layer (s_f); this is shown as a chained line. Again this curve applies to the case when the coarse layer is just coolable by boiling.

As the heat flux in the bed at any height is proportional to the height, and the heat flux must be continuous at the interface, the diagram may be used to determine which combinations of coarse and fine layers can just be cooled by boiling. This is achieved in the following way (note that the diagram is for a fixed volumetric heating rate):

> A depth of coarse layer z_c is chosen, and the values of s_c and s_f corresponding to this depth are found. The saturation profile for the fine layer (solid line) is then followed from (s_f, z_c) until it intercepts the line s = 1 at height z_t, say, which is the total depth of the layer that is just coolable by boiling. The saturation profile for this case simply follows the dashed line up to the interface at (s_c, z_c) and then the solid line (not necessarily illustrated) from (s_f, z_c) to (s = 1, z_t).

It is seen that there is a range of values of z_c from 0 to almost z_f (the depth of fines alone that can be just cooled by boiling) for which the total depth of the two layers that is just coolable by boiling is less than z_f. Whereas z_f = 0.37m, the minimum value of z_t = 0.13m, which occurs for z_c = 0.12m. Similar diagrams can be drawn for any combination of particle sizes and volumetric heating rate. Because of the shape of the capillary pressure function all such systems will show a similar behaviour.

.2. Comparison calculations for layered and graded beds

When the particles are graded in height there are no jumps in saturation. If the mean particle diameter decreases with height one obtains, as noted by Lipinski [9], a term on the RHS of equation (7) that tends to impede the flow. However the total capillary pressure gradient is on average still favourable to drawing liquid into the bed, so that apart from the mal-distribution of the capillary pressure gradient across the bed one would expect the dryout heat flux of the graded bed to be at least Φ_F (the dryout heat flux of a uniform debris bed consisting of the fine top layer particles only in the limit when capillary forces become negligible).

Example calculations for water at 1 bar are shown in Figure 3. These show the variation in dryout heat flux with bed height for the following debris bed configurations

- (i) 0.004m particles (coarse) only
- (ii) 0.0012m particles (fine) only
- (iii) 0.06m coarse superposed by a depth of fine particles
- (iv) a uniform gradient in particle diameter between coarse particles at the bottom and fine particles at the top
- (v) 0.06m coarse layer superposed by a uniform gradient in particle diameter from coarse to fine
- (vi) as (iii) but with no heating in the fine layer. This corresponds more closely to the effect of the heating method used in [13].

In all cases $\varepsilon = 0.42$ throughout the bed. The limits as the bed depth is increased in (i) and (ii) are denoted Φ_C and Φ_F.

It is seen that the graded beds considered do have dryout heat fluxes lying between Φ_F and that of a similar bed consisting of fine particles alone, except where the gradation is very gradual in which case the dryout heat flux marginally exceeds that of the fine bed of the same depth. The reduction in dryout heat flux is greater when the gradation is confined to the upper part of the bed.

The two layer beds (iii) and (vi) show the much greater reduction when there is a discontinuity in particle size that forces a jump in saturation. The lowest dryout heat fluxes are found for the case where the heating is concentrated in the lower coarse layer (vi), for which a limiting heat flux, Φ_S, as the depth of fines is increased, of less than one-half that of the fines alone is predicted.

A detailed analysis of equation (7), in particular of the locations of the zeros of $ds/d\xi$, shows that Φ_S can be at most Φ_F. For the particular coolant and bed data considered in Figure 3, the diameter of the fine particles would have to be at least 3.1mm, when the diameter of the coarse particles is 4mm, for Φ_S to equal Φ_F.

The results obtained for (vi) agree qualitatively with the experimental results [13], but the values of the limit on the dryout heat flux differ by about a factor of 5, compared with a factor of about 2, for cases (i) and (ii). The additional reduction may be due to a reduction in porosity close to the interface or may suggest the need to modify the capillary pressure function. Both the experimental and the calculated results become reasonably close to the respective limits when the depth of unheated particles is about 20mm.

4. THE APPROACH TO DRYOUT WHEN CAPILLARY PRESSURE EFFECTS ARE SMALL

4.1 General considerations

We now consider the transient behaviour predicted by the boiling model. It was seen in Section 2.2 that for millimetre-sized particles in water the parameter determining the importance of capillary pressure, E,

is small. Equations (5) to (7) usually give a second order quasi-linear partial differential equation for s of parabolic form. However when capillary pressure effects are neglected (E = 0) this reduces to first order, and becomes hyperbolic. In this case the method of characteristics (see e.g. [17] may be used to obtain solutions.

The characteristic equations are found by considering V_v and V_ℓ to be functions of s and ξ. For constant qo and f = 1 they are

$$\frac{d\xi}{d} = \frac{g_1}{g_2} \text{ and } \frac{ds}{d\tau} = \frac{g_3}{g_2} - 1$$

where $$g_1 = V_v\left[\frac{\partial}{\partial s}\left(\frac{1}{\phi_v}\right) + A|V_v|\frac{\partial}{\partial s}\left(\frac{1}{(1-s)\phi_v}\right)\right] - \frac{V_\ell}{C}\left[\frac{\partial}{\partial s}\left(\frac{1}{\phi_\ell}\right) + \frac{A|V_\ell|}{B}\frac{\partial}{\partial s}\left(\frac{1}{s\phi_\ell}\right)\right]$$

$$g_2 = \frac{1}{\phi_v}\left[1 + \frac{2A|V_v|}{1-s}\right] + \frac{1}{C\phi_\ell}\left[1 + \frac{2A|V_\ell|}{Bs}\right]$$

and $$g_3 = \frac{(1 - BC)}{C\phi_\ell}\left[1 + \frac{2A|V_\ell|}{Bs}\right]$$

It may also be shown that

$$V_v = \xi - \xi^o$$

along a characteristic where ξ^o is the constant of integration. If the characteristics start from the bottom of the bed $\xi^o = 0$; otherwise ξ^o is determined by the initial conditions.

Solutions of the characteristic equations have the following properties

(i) s decreases monotonically along a characteristic

(ii) characteristics starting at the bottom of the bed at time τ_o all satisfy a single equation $H(\xi, \tau - \tau_o) = 0$ for $\tau > \tau_o$. Thus in the region covered by these characteristics $\partial s/\partial\tau = 0$

(iii) the only boundary condition acceptable at $\xi = 0$ (bottom of the bed) is s = 1

(iv) if the bed is initially saturated with liquid a top boundary condition is not required during the early part of the transient, however in some circumstances if the bed is uncoolable a top boundary condition will be required at some stage

(v) if the heating rate changes at $\tau = 0$ or the bed is initially fully saturated there will be discontinuities in the partial derivatives of liquid saturation across the characteristic passing through $\xi = \tau = 0$.

When E is small, but non-zero, boundary layer analysis shows that instead of the discontinuity (v, above) there is a thin layer around the characteristic across which the partial derivatives change very rapidly. Further if E is non-zero an upper boundary condition is always required. This matches on to the E = 0 solution through a boundary layer at the top of the bed.

When a top boundary condition is required for E = 0 (iv, above) it may be obtained by analysis of the boundary layer that does form at the top of the bed in the case of small non-zero E; this boundary layer matches the solution of the hyperbolic equations to the top boundary condition (usually s = 1). However the limiting condition for $E \to 0$ is <u>not</u> S = 1 (see below).

To pursue the analysis of solutions when E = 0 further, three cases must be considered:

(i) bed coolable

(ii) bed uncoolable and $V^o \geq V^* = BC(\sqrt{1 + 4A} - 1)/2A$

(iii) bed uncoolable and $V^o < V^*$

4.2. Bed coolable

As the bed is coolable a steady state solution exists It is achieved in a finite time, satisfies s = 1 at the bottom of the bed, and no upper boundary condition is required.

4.3 Bed uncoolable and $V^o \geq V^*$

Characteristics are such that ξ increases monotonically with τ. Dryout is assumed to occur when and where s = 0 is first reached. If fluid inertia effects are negligible (A = 0) $\partial s/\partial\xi$ is zero in the upper part of the bed and dryout first occurs in the region $\xi \geq V^o/(BC)$.

4.4 Bed uncoolable and $V^o < V^*$

The characteristic through $\xi = \tau = 0$ has a turning point at which $d\xi/d\tau = 0$, occurring at $\xi = \xi_D < \xi_m$, where ξ_m is the non-dimensional bed depth and ξ_D corresponds to the maximum depth of a stable boiling layer. As characteristics starting from $\xi = 0$ and some $\tau > 0$ are just translations, along the τ axis, o the characteristic passing through $\xi = \tau = 0$ the solution for s will break down, through characteristics crossing, before s has fallen to zero. This breakdown may be resolved by introducing a discontinuity in saturation, mathematically analagous to a shock. It appears at ξ_D and propagates downwards; below it the saturation profile is identical to the steady state solution that would have been obtained if the bed had been sufficiently shallow to be coolable; above it the saturation is lower and decreasing with time. If Y is the (non-dimensional) position of the shock at (non-dimensional) time T, the position of the interface is given by

$$\frac{dY}{dT} = -\frac{[V_v]}{[s]}$$

where [ ] are used to denote the jump across the interface.

To continue the analysis further, attention is restricted to A = 0 (inertia effects negligible). It is found that three possible situations arise, two of these being illustrated in Figure 4, in which B = 0.0144, C = 0.0434 (for water at 1 bar) N = 1 and $V^o = 0$. In Figure 4a the region in which dryout starts extends from the shock to the top of the bed (situation A), but in Figure 4b the region in which dryout starts, although still having its lowest point on the shock, does not extend to the top of the bed (situation B). The third situation arises for a shallower, but still uncoolable bed, in which dryout initially occurs at a point on the shock, rather than over a region of the bed (situation C).

In situation A no boundary condition is ever require at the top of the bed. In the other two situations there exists a characteristic for which the line $\xi = \xi_m$, in ξ, τ space, is tangential. Let the value of s and τ where this characteristic touches the top

of the bed be s_m and τ_m respectively. No top boundary condition is required while $\tau < \tau_m$. However once $\tau \geqslant \tau_m$ a top boundary condition is required. By considering the boundary layer at the top of the bed when E is small but non-zero it can be shown that the boundary condition required when E = 0 is

$$s = s_m \text{ at } \xi = \xi_m \text{ when } \tau \geqslant \tau_m.$$

Further, for situations A and B the (non-dimensional) time to dryout is independent of the (non-dimensional) bed depth and the efflux through the bottom of the bed, and is the same as for the case described in section 4.3. The region in which dryout first occurs is, however, a function of the efflux through the bottom of the bed. For situation C the (non-dimensional) time to dryout increases and the (non-dimensional) position of dryout decreases as the (non-dimensional) bed depth is reduced.

4.5. Comparison with experiments and other theoretical work

Compared with the number of experimental studies of dryout heat fluxes, relatively little work has been done on time dependent phenomena in debris beds as they approach dryout.

However, in one set of experiments the approach to dryout has been observed [14]. Before dryout occurred an interface was seen. Below this interface there was heavily boiling liquid, but above it the liquid saturation was low. The interface moved down the bed with time. These observations are (qualitatively) explained by the results given in section 3.3, where the shock-like discontinuity in liquid saturation is the model analogue of the experimentally observed interface. Results in section 4.4 also (qualitatively) explain the observed locations of the onset of dryout.

Bergeron [18] has also developed a transient model. The model does not include capillary pressure effects and also neglects some small terms included in the equations developed here. The results discussed above are in general agreement with [18], differences being attributable to the small terms that we include but Bergeron neglects.

. THE INCLUSION OF A DRIED-OUT LAYER

As noted in the introduction the models described so far cannot be applied for the whole region once dryout has occurred. However, the equations given in section 2 should still apply to any region of the bed in which there is two phase coolant flow.

.1. Steady state considerations

Lipinski [9] argues that, in the steady state, the heat flux is a known function of height, so the saturation profiles may be calculated by integrating downwards from the top of the bed. At some height the condition s = 0 may be reached, and according to Lipinski this gives the equilibrium thickness of the boiling region. Below this, in the dried-out region, heat transfer is predominantly by conduction. At the interface between the dried-out region and the boiling region this conducted heat flux is used to boil liquid coolant and produce a flux of vapour through the boiling region. Because s = 0 at the interface in the model calculations, it is possible that vaporisation may spread over a finite thickness of the bed; however the saturation profiles for 1.2mm diameter particles in Figure 2 do show that non-neglible values of s occur close to the bottom of the boiling layer.

Attempts to include a finite vaporisation layer in the model analogous to the condensation layer described in [19] have not proved successful because of the unphysical forms required for the heat transfer coefficient between the heated particles (with vapour at the particles' temperature) and the liquid assumed to be at the boiling point. Once s > 0 the model would require that at least all the local volumetric heating is taken up by the liquid. Below we use the interface description based on Lipinski's work.

The steady-state maximum temperature T_m in the bed can be found using

$$T_m = T_b + q\, z_D^2/2k_e$$

where T_b is the boiling point of water, k_e is the effective thermal conductivity of the bed and z_D is the depth of the dried-out region. An adiabatic base has been assumed here, and in the calculations described below. At temperatures of interest the conductivity of the debris is $\sim 3\ W\ m^{-1}\ K^{-1}$ whilst that of steam at 1 bar is $0.025\ W\ m^{-1}\ K^{-1}$ at 100 C, but $0.135\ W\ m^{-1}\ K^{-1}$ at 1000 C. Limits on the bed conductivity can be found [20]; at 1000 C these are $0.5\ W\ m^{-1}\ K^{-1} \leqslant k_e \leqslant 1.5\ W\ m^{-1}\ K^{-1}$, where $\varepsilon = 0.42$ has been assumed. Because of the lack of connectivity of the more conductive phase k_e is likely to lie between the lower limit and the estimate of effective medium theory [20] which in this case is $1.1\ W\ m^{-1}\ K^{-1}$. Taking $q = 2 \times 10^6\ W\ m^{-3}$ (as assumed for Figure 2 and used in all calculations below) and $k_e = 1\ W\ m^{-1}\ K^{-1}$ it is found that unless z_D is less than 0.05m the maximum bed temperature in the steady-state will reach the melting point of the fuel.

5.2. Transient Modelling

The heat-up rate of debris without any cooling is simply given by $q/(\rho_d\ c_d(1 - \varepsilon))$, where the subscript d here denotes debris properties. Taking $\rho_d = 10^4\ kg\ m^{-3}$ and $c_d = 600\ J\ kg^{-1}\ K^{-1}$, this is $0.57\ C\ s^{-1}$. Thus to heat the bed from 100 C to the melting point of the debris would take over 4000s. One can compare this with the time required to set-up a steady-state boiling profile. Using Figure 4 it is seen that dryout is reached when τ, the non-dimensional time is about 80; this corresponds for water at 1 bar to a time of 23s. At this time the steady-state profile with s = 1 at the top of the bed and s = 0 at the bottom of the boiling layer has not been achieved, and the modelling of this transition is incomplete; however it is likely to occur on a similar timescale. Further adjustments to the saturation profile as the heat flux from the dried-out zone varies are also likely to occur on much shorter timescales than that for the heat-up of the dried-out zone. Thus one may assume steady state behaviour in the boiling region, but consider transient behaviour in the dried-out region.

For a given bed it is easiest to use an approximate analytic form for the heat transfer characteristics of the boiling region. One such form which reflects the constant gravity head and the dependence on thickness of the capillary pressure term is

$$\Phi = \Phi^o\left(1 + \frac{z^c}{z_b}\right) \qquad (10)$$

where Φ is the heat flux through the top of the layer, z_b is the thickness of the boiling region, and Φ^o and z^c are constants to be fitted to the

detailed calculations. The magnitude of z^c is determined by the importance of the capillary pressure: if E = 0 then $z^c = 0$ and indicates that in this limit the boiling region would vanish if the heat flux to be removed is greater than Φ^o. For E > 0, z^c is also greater than zero so the boiling region has a finite thickness. The form of equation (10) is most appropriate for A << 1, and other functional forms may give better fits; however for the fine particles ($d = 1.2 \times 10^{-3}$m) of Figure 2 (A = 1.4) the values $\Phi^o = 6.54 \times 10^5$ W m^{-2} and $z^c = 4.25 \times 10^{-3}$m do fit the data for Φ from 7.5×10^5 W m^{-2} (dryout) to $= 4 \times 10^6$ W m^{-2} to better than 10%. These values are used below.

Assuming that the debris was quenched initially and that the final bed is not coolable by boiling because of the ensuing accumulation of debris, there will be no heat flux from the dried-out region to the boiling region at the start of the transient (t = 0). Thus at t = 0, $\Phi = q\, z_b$ and the boiling layer has the same depth as the bed with the same q that would just be coolable by boiling. Φ gradually increases as the conduction profile in the bed builds up. The transient equation for temperature is

$$(1 - \varepsilon)\rho_d\, c_d \frac{\partial T}{\partial t} = \frac{\partial}{\partial z}\left(k_e \frac{\partial T}{\partial z}\right) + q \;;\; z<h-z_b \qquad (11)$$

with boundary conditions $\partial T/\partial z = 0$ if the lowest surface is adiabatic, and $-k_e(\partial T/\partial z) = \Phi - q\, z_b$ at $z=h-z_b$, where h is the height of the bed. Equations (10) and (11) form a coupled system of equations that determine z_b. The solution of equation (2) gives

$$-k_e \frac{\partial T}{\partial z}\bigg|_{z=h-z_b} = q(k_e t/(\rho_d c_d(1-\varepsilon)))^{\frac{1}{2}} \qquad (12)$$

where $G(t) \approx 1$ for $t < (\rho_d\, c_d(1-\varepsilon)(h-z_b)^2/k_e)$.

Substituting (12) into (10) implies

$$(k_e t/(\rho_d c_d(1-\varepsilon)))^{\frac{1}{2}} G(t) + q\, z_b = \Phi^o\left(1 + \frac{z^c}{z_b}\right) \qquad (13)$$

Taking G(t) = 1 in the example calculations it is found that $z_b = 0.34$ at t = 0. This is only reduced to $z_b = 0.31$ at t = 4200s, the time at which melting of the debris would be expected to start, irrespective of the value of h provided it is greater than 0.40m to satisfy the condition on G(t).

Thus while the debris remains solid the boiling layer is likely to have a similar thickness to that of the depth of bed which is just coolable by boiling for the same heating rate, not that predicted by the steady-state model. The bulk of the heat generated in the dried-out zone raises the temperature of that region and is not used to generate steam. Thus the steaming rate is only marginally enhanced over that from the bed which is just coolable. The transient model described here can be extended for other boundary conditions provided there is no gas generation from below (e.g. because of concrete decomposition).

CONCLUSIONS

In this paper we have described various developments and applications of the model for boiling and dryout in debris beds based on conservation laws and the phenomenological equations for flow in a porous media. These include

(i) the equations being developed in full vector form for variable particle diameter and volumetric heating rate,

(ii) an investigation of the conditions in which capillary effects determine the jumps in saturation in a multi-layered bed,

(iii) a detailed consideration of why the dryout heat flux from a two-layered bed may be considerably less than that of particles of the finest layer alone,

(iv) a comparison that shows that gradations in particle size have much less effect in reducing dryout heat fluxes than stratifications. The depression of dryout heat flux is largest for the heating method used in [13],

(v) the use of characteristics to predict the dependence of saturation on time for beds in which capillary effects are small. In certain circumstances in which the bed eventually dries out, a discontinuity in saturation arises before dryout occurs, as observed in Hofmann's experiments [14],

(vi) an investigation which showed there were difficulties in introducing a vaporisation layer analogous to the condensation layer previously used by the authors, and

(vii) the development of a simple transient model for the post-dryout behaviour of a bed of initially quenched particles. This showed that while the debris is still solid, most of the heat generated in the dried-out zone raises the local temperature; the thickness of the boiling zone is close to the bed depth that is just coolable by boiling, rather than that predicted by the steady-state model.

ACKNOWLEDGEMENTS

This work was supported by the Safety and Reliability Directorate, Culcheth. The authors thank Drs F Briscoe and R S Peckover for advice on the preparation of this paper, and J Morgan, J Wheatley and A Wilmore for assistance with computations.

Figure 1. Two-Layered Bed.

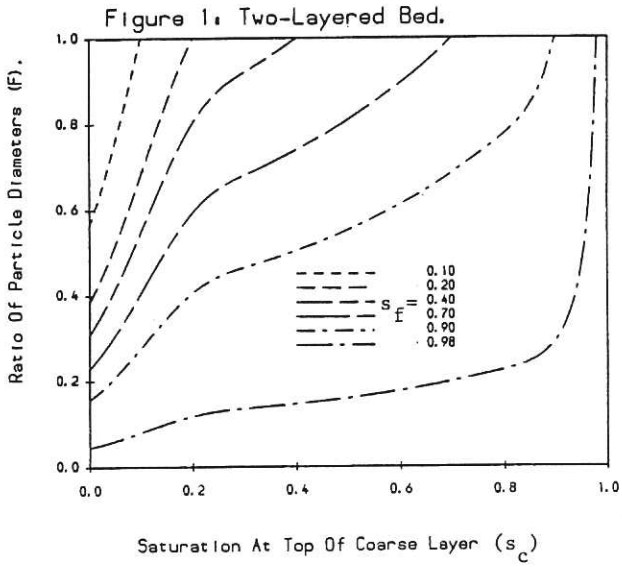

REFERENCES

1. Zion Probabilistic Safey Study. Commonwealth Edison Co. Docket No. 50-295 (1981).

2. Sizewell B Probabilistic Safety Study, Westinghouse Electric Corp., WCAP-9991 (1982).

3. R Trenberth & G F Stevens. An experimental study of boiling heat transfer and dryout in heated particulate beds. AEE Winfrith report AEEW-R1342 (1980).

4. L Barleon & H Werle. Dependence of dryout heat flux on particle diameter for volume- and bottom- heated debris beds. Kernforschungzentrum Karlsruhe, KfK 3138 (1981).

5. D Squarer, L E Hochreiter & A T Pieczynski. Some aspects of decay heat removal from a debris bed and its implication to degraded core coolability. In 'Post accident debris cooling' (U Muller & C Gunther, eds.), p159-164. G Braun, Karlsruhe (1983).

6. H C Hardee & R H Nilson. Natural convection in porous media with heat generation. Nucl. Sci. and Eng., 63, 119-132 (1977).

7. R J Lipinski. A one-dimensional particle bed dryout model. Trans. Amer. Nucl. Soc. 35, 358-360 (1980).

8. G L Shires & G F Stevens. Dryout during boiling in heated particulate beds. AEE Winfrith report AEEW-M1779 (1980).

9. R J Lipinski. A model for boiling and dryout in particle beds. Sandia Laboratories report SAND82-0765 (NUREG/CR-2646) (1982).

10. B D Turland & K Moore. One-dimensional models of boiling and dryout. In 'Post accident debris cooling' (U Muller & C Gunther, eds.), p192-197. G Braun, Karlsruhe (1983).

11. T Ginsberg, J Klein, J Klages, C E Schwarz & J C Chen. Phenomenology of transient debris bed heat removal. In 'Post accident debris cooling' (U Muller & C Gunther, eds.), p151-158. G Braun, Karlsruhe (1983).

12. D H Cho, D R Armstrong, L Bova, S H Chan & G R Thomas. Experiments on quenching of a hot debris bed. In 'Post accident debris cooling' (U Muller & C Gunther, eds.), p145-150. G Braun, Karlsruhe (1983).

13. G F Stevens & R Trenberth. Experimental studies of boiling heat transfer and dry-out in heat generating particulate beds in water at 1 bar. In 'Post accident debris cooling' (U Muller & C Gunther, eds.), p108-113. G Braun, Karlsruhe (1983).

14. G Hofmann. On the location and mechanisms of dryout in top-fed and bottom-fed beds. In 'Post accident debris cooling' (U Muller & C Gunther, eds.), p186-191. G Braun, Karlsruhe (1983).

15. A E Scheidegger. The physics of flow through porous media. Univ. of Toronto Press (1974).

16. F A L Dullien. Porous media - Fluid transport and pore structure. Academic Press (1979).

17. C-Y Chow. An introduction to computational fluid mechanics. John Wiley & Sons (1979).

18. E Gorham-Bergeron. A one-dimensional time-dependent debris bed model. Paper presented at the ASME - JSME Thermal Engineering Joint Conference, Honolulu (1983).

19. B D Turland & K Moore. Debris bed heat transfer with top and bottom cooling. Paper presented at 21st ASME/AIChE Heat Transfer Conference, Seattle, July 1983.

20. I Cook & R S Peckover. Effective thermal conductivity of debris beds. In 'Post accident debris cooling' (U Muller & C Gunther, eds.), p40-45. G Braun, Karlsruhe (1983).

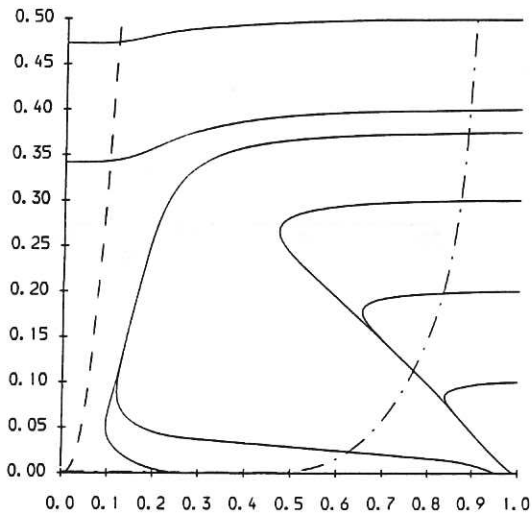

Fig 2. Vertical axis: height in bed (metres)
Horizontal axis: saturation
See section 3.1 for discussion

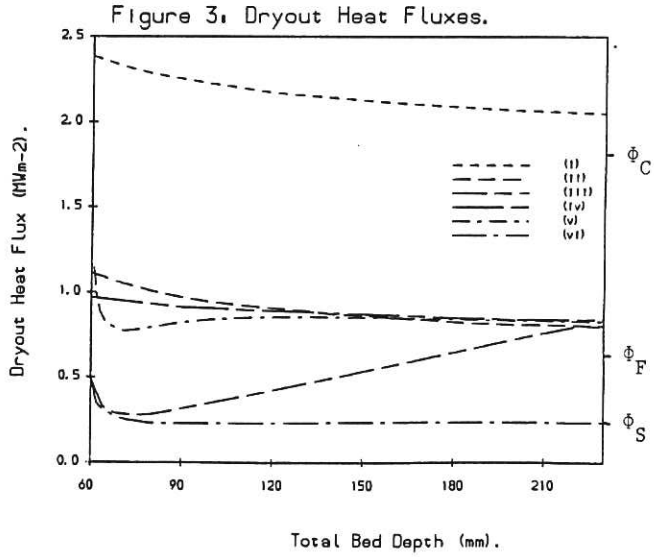

Fig 3. See section 3.2 for description of cases

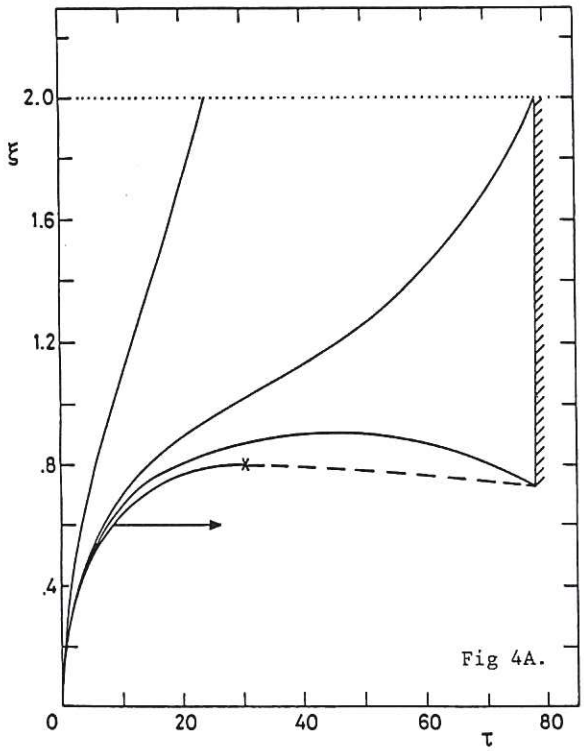

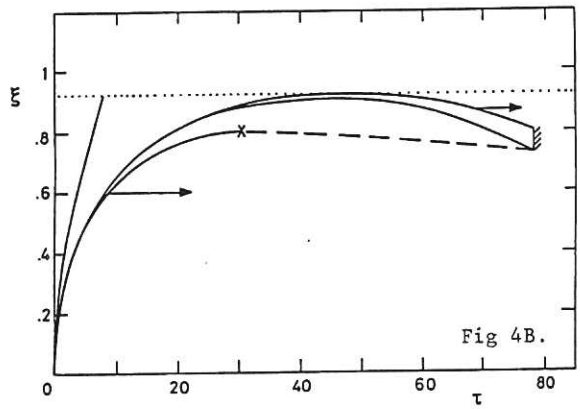

Fig 4 The onset of dryout in the no-capillary pressure limit. The bed is assummed fully saturated at $\tau = 0$. The solid lines denote characteristics (all those shown start close to the bottom of the bed at $\tau = 0$). The dotted line denotes the top of the bed ($\xi = 2$ in Fig 4A and $\xi = 0.92$ in Fig 4B). The arrow denotes that the characteristics in the region to the right are merely translations of that drawn. The discontinuity in saturation starts at point X and propagates along the broken line. The bed dries out initially over the region indicated by the hatching. The calculations are for water at 1 bar, with $A = V^{o} = 0$ and $N = 1$.